Recognition of Hand Gestures using Wavelet Packet Transform and Cascaded Feed Forward Neural Networks

Mary Vasanthi S (vasanthi@sxcce.edu.in)
St Xavier's Catholic College of Engineering https://orcid.org/0000-0002-9745-6922
T Jayasree
Government College of Engineering Tirunelveli

Research Article

Keywords: Signal processing, Electromyogram, Discrete wavelet transform, Feature extraction, Pattern recognition, Feed Forward Neural Network.

Posted Date: January 19th, 2023

DOI: https://doi.org/10.21203/rs.3.rs-1977270/v1

Recognition of Hand Gestures using Wavelet Packet Transform and Cascaded Feed Forward Neural Networks

Mary Vasanthi S[1*], Jayasree T [2], Haiter Lenin A[3]

[1 *]*Department of Electronics and Communication Engineering, St Xavier's Catholic College of Engineering, Nagercoil, Tamilnadu, India. Email: vasanthi@sxcce.edu.in*

[2]*Department of Electronics and Communication Engineering, Government College of Engineering, Tirunelveli, Tamilnadu, India. Email: jayasree@gcetly.ac.in*

[3]*School of Mechanical and Chemical Engineering, WOLLO University, Kombolcha Institute of Technology, Kombolcha, Ethiopia, Post box no: 208.E-mail: drahlenin@kiot.edu.et*

Corresponding Author Email :[1] vasanthi@sxcce.edu.in*

ABSTRACT

This paper presents a noval framework that classifies finger movements automatically using Wavelet Transform and its derivatives by capturing statistical features from the discrete time Electromyogram (EMG) signals. In the suggested method, wavelet-based denoising is used to separate out the subject's EMG signals, and then Discrete Wavelet Transform (DWT) and Wavelet Packet Transform are used to decompose the signals and extract their key characteristics (WPT). The derivatives of the feature sets are employed to analyse the correlation among them. This method is motivated by the surveillance that there exists a distinctive correlation between the different features of the samples of the signals extracted at various frequency levels. Experimentally, it was perceived that this correlation varies from signal to signal. Both Feed forward and Cascaded Feed forward Artificial Neural Networks (ANN) are used for classification. Experiments show that the proposed method significantly improves the classification rate. The performance of the suggested wavelet-based features and their derivatives in combination with ANN and trained with the Levenberg-Marquardt algorithm was evaluated by comparing the simulation results for various sets of features. Comparing the new method benefits to earlier traditional methods in terms of classification performance helped to further highlight their advantages. These experimental findings demonstrate that the suggested approach performs admirably in classifying finger movements based on EMG signal patterns. The suggested methodology also helps clinicians increase the reliability of myoelectric pattern recognition.

Index Terms- Signal processing, Electromyogram, Discrete wavelet transform, Feature extraction, Pattern recognition, Feed Forward Neural Network.

1 INTRODUCTION

For a person, who loss the limb after an injury, an artificial hand is needed to carry out his daily activities. Today's highly sophisticated prosthetic hands offer individual finger movement. These prosthetic hands are controlled using surface Electromyogram (EMG) signals, which are retrieved during the electrical activity of muscles. The myoelectric control systems rely on a pattern recognition approach that entails recording of EMG signals from several channels, extracting features from the signals, and categorising the features using the proper classifiers [1, 2]. EMG signal is not periodic. Additionally, it is complicated in nature and can occasionally even be contradictory because it can be altered by a number of factors such muscle fatigue, electrode displacement, sweat, and changing skin thickness. The EMG signal carries a significant quantity of data about limb movements and functionality despite its complexity. As a result, it can be successfully used in prosthetic [3, 4], rehabilitation or clinical posture analysis and diagnosis of neuromuscular illnesses [5- 7].

Furthermore, EMG is a pathetic bio-signal corrupted by the noise from the internal cross-talk, ambient electromagnetic radiation, and movement artefacts. Different types of filtering techniques are employed to remove various noise embedded in the EMG signal. Notch filters were applied to remove the high-frequency noise present in the signal [8]. One of the shortcomings of notch filter design is that the maximum value of the output below the notch frequency is usually less than the maximum value of output above the notch frequency. To remove movement artefacts and power line interferences, Butterworth low pass and high pass filters are employed [9-11]. Nevertheless, the major problem of low pass and high pass filters is that, they sieve the DC offset of the signal and unwanted ripples that are produced at certain frequencies [12].However, Wavelet-based denoising provides fine frequency resolution at high frequencies [13]. Consequently, noise components in the desired signal can be easily isolated by preserving important high-frequency transients.

The success of myoelectric pattern recognition depends on the features that are extracted and the classifier that is used [14]. The variables taken into account in the time-domain typically have a lot of relevance. Different motion recognition techniques have been applied to a range of time-domain features that have been proposed. Riilloet.al [15] utilised five different hand movements and seven separate time-domain features. Nianfeng Wang [16] proposed eight hand gestures classification using time-domain and Autoregressive (AR) coefficients. Khushabaet.al [17] suggested three levels of time-domain Power Spectral Descriptors (TD-PSD) for the detection of wrist and hand movements. In reality, thorough consideration of the time-domain aspects in EMG analysis is required to minimise the time delay and produce effective controllability in real-world applications. Iker Mesaet.al [18] used frequency-domain features along with Support Vector Machine (SVM) classifier for the recognition of hand gestures. The properties of the energy/entropy distribution are used to select the nonlinear characteristics of the signal [19]. Prashar et.al [20] employed time and frequency domain-based statistical characteristics and the empirical mode decomposition (EMD) method to classify signals. An-Chih Tsai et.al [21] built a pattern recognition model using SVM classifier and Principal

Component Analysis (PCA). For the analysis of hand movement, spectral-based features and a Linear Discriminant Analysis (LDA) classifier were developed. [22-24]. However, this approach required more processing time. Wavelet transform is a potent time-frequency mathematical tool that has been used in many areas of biosignal processing, including EMG. [25, 26].

The classification of EMG signals served as the foundation for the development of myoelectric prosthesis control systems [27-29]. Due to the EMG signal's significant interference and fluctuation, classifying EMG signals is a challenging pattern recognition task [30-32]. ErconGokgozet.al [33] proposed the Decision Tree Algorithm (DTA) and Discrete Wavelet Transform (DWT) combination for classifying biological signals. FirasAlomariet.al [34] proposed a pattern recognition system using the energy of wavelet coefficients to categorise eight different hand gestures. In [35, 36], an Artificial Neural Network (ANN) was trained using information on the level of muscular contraction and previous classifier outputs in order to determine the accuracy of the classifier's decision., YinaGuoet.al [37] used ANN to categorise six different hand movements and achieved excellent accuracy, however the system was not resilient when amputees' electrodes were shifted, changed in size, or oriented differently.

The removal of noises embedded in the EMG signals is done using wavelet-based denoising algorithms. The EMG signal is processed using the Wavelet Packet Transform (WPT) and DWT to extract various features. Calculating non-linear measurements allows one to estimate the signal's non-linear characteristics. These attributes can be utilised as input data for an ANN classifier, which can categorise different finger movements, because it has been found that they are significantly different for different finger movements. The remaining paper is organized as follows: In the next section, we give information about the methodology of the proposed framework. Section 3 provides subjects and presents the methods applied in each step of the EMG signal classification process. It also gives a complete experimental study of the feed forward pattern recognition network model based EMG signal classification scheme. Results and Discussions are given in section 4. Finally, the conclusions are summarized in section 5.

2 Methodology

Figure 1 illustrates the three modules of the proposed methodology for an automated finger motion identification system: data collection and pre-processing, feature extraction, and an ANN-based classification system. The sensors first identify and record the EMG signals of the forearm muscles and further pre-processed to remove artefacts. The recorded signals are the discrete samples of size between 10,000 and 20,000 for a typical movement. The representation of EMG signals in terms of samples increase the complexity of the classification task, which requires dimensionality reduction. This reduction leads to represent the EMG signal in terms of a feature vector.

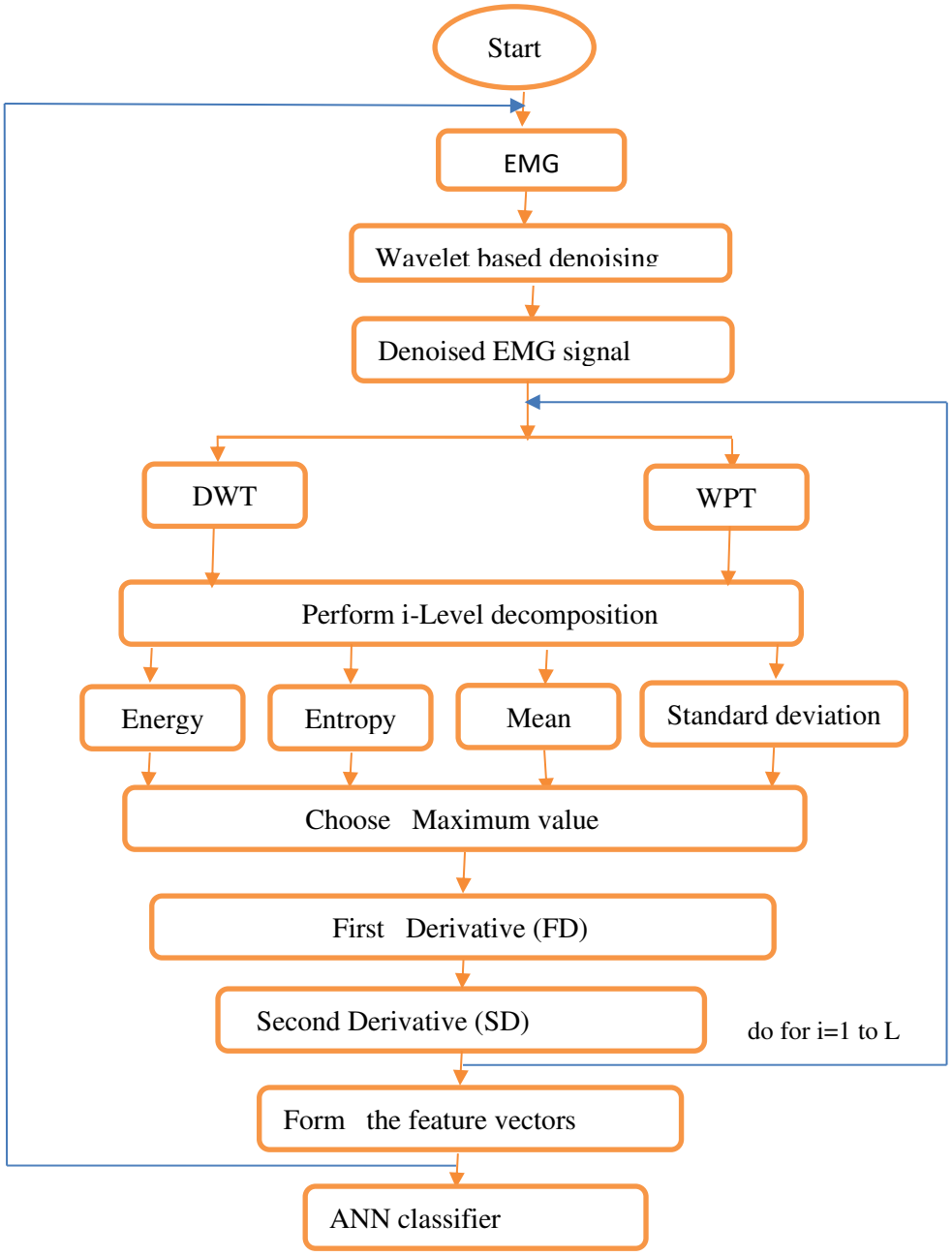

Figure1Electromyogram based finger motion recognition system

The decomposition of the original EMG signal into signal components at various frequencies using DWT and WPT results in a transformation in the time-frequency domain that allows for the feature extraction from the original EMG signal. The pattern vector, or original waveform, should be reduced by a feature extractor to a lower aspect, which holds the majority of the valuable data from the original signal. The identification of patterns and regularities in data is the focus of the machine learning technique known as ANN-based classification. The statistical or non-statistical nature of the pattern classification technique will depend on whether the learning is supervised or unsupervised.

a) Experimental setup: A group of ten volunteers six males and four females, aged between 20-38, free of any muscular/neurological disorders participated in the experiment. As indicated in Figure 2, subjects were seated in an armchair with one end of their arm fixed so that they could perform hand movements freely without any constraints. Ag/AgCl disposable surface electrodes were positioned at equidistance on the subject's right forearm to collect the EMG data. Each subject's wrist was attached to a conductive adhesive reference electrode (Dermatrode Reference Electrode). The signals were digitally connected (24 bit A/D converter) and sampled at 2 kHz before being stored for offline analysis in the MATLAB environment.

Figure 2Experimental setup for data acquisition

The experimental protocol comprised 10 finger movements namely Hand close(HC),Thumb(T),Index(I),Little(L),Middle(M),Ring(R),Thumb-Index(TI),Thumb-Middle (TM), Thumb-Ring(TR) and Thumb-Little(TL)were selected and they are shown in Figure3. The subjects performed each motion in 6 trials and recorded for 4 sec.

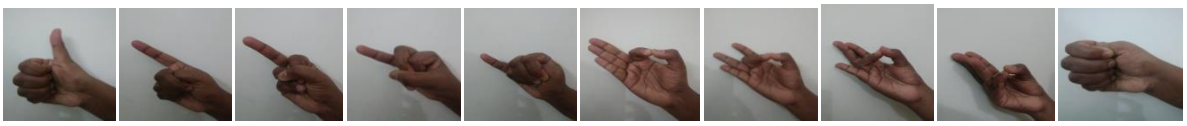

(a)T (b) I (c) M (d) R (e) L (f) TI (g) TM (h) TR (i)TL (j) HC

Figure 3 Waveforms for finger motions

b) Wavelet denoising: The very sensitive nature of EMG signals leads to the contamination of various types of noise sources which would contribute to very deprived classification results. Wavelet denoising takes advantage of the fact that some signal features are related to the signal's average power and others are related to the noise value. Therefore, if the noise-related details are filtered, the

signal can be reconstructed using other details without losing any of the signal's content. Therefore, choosing the right threshold algorithm and threshold scaling function is crucial. Let us suppose the signal x_i be corrupted with Additive White Gaussian noise. The noisy input signal is given by

$$y_i = x_i + \sigma\varepsilon_i, i = 1,2,.....2^m \tag{1}$$

The noisy signal can be decomposed to obtain discrete wavelet coefficients $S(a,b)$, where a and b are the time-scale parameters. Determine a threshold $\lambda = u\{S(a,b)\}$ based on the following threshold rules to get the modified coefficients $Z(a,b) = D\{S(a,d),\lambda\}$

i)Rigrsure: Suppose $W = [w_1, w_2, w_3.....w_N]$ is a vector made up of the squares of the wavelet coefficients from small to large. Choose the smallest value from the risk vector:

$$R = \{r_i\}_{i=1,2.....N} = \frac{N - 2i + (N-i)w_i + \sum_{k=1}^{l} w_k]}{N} \tag{2}$$

The selected threshold is $\lambda = \sigma\sqrt{w_b}$, where, w_b is the b^{th} squared wavelet coefficient (coefficient at minimum risk) chosen from the vector and σ is the standard deviation of the noisy signal. [13].

ii)Sqtwolog: The threshold values *(λ)* are calculated using universal threshold (square root log) method given by, $\lambda_j = \sigma_j\sqrt{2\log(N_j)}$, where N_j is the length of the noisy signal at j^{th} scale and σ_j is Median Absolute Deviation (MAD) at j^{th} scale, $\sigma_j = \frac{MAD_j}{0.6745}$ (3)

iii)Heursure: If λ_1 and λ_2 represent threshold obtained from Sqtwolog and Rigrsure respectively, then, $\lambda = \begin{cases} \lambda_1, & A > B \\ \min(\lambda_1, \lambda_2), & A \geq B \end{cases}$, where $A = \frac{S-N}{N}$ and $B = (\log_2 N)^{3/2}\sqrt{N}$ (4)

where S is the sum of the squared wavelet coefficients, and N is the length of the wavelet coefficient vector.

iv)Minimaxi: The threshold, $\lambda = \begin{cases} \sigma(0.3936 + 0.1829\ \log_2 N), & N > 32 \\ 0 & N < 32 \end{cases}$, $\sigma = median\frac{|w|}{0.6745}$.

Finally, Inverse Discrete Wavelet Transform is found out for the modified wavelet coefficient in order to get the denoised signal.

Feature extraction is an essential stage for pattern recognition. As indicated by earlier studies on EMG pattern recognition, wavelet features can be helpful [38], DWT and WPT features were adopted in this study. The feature set includes more statics namely Energy, mean, Standard deviation, and entropy.

c) Discrete Wavelet Transform: The features of the signal can be extracted by decomposing the input signal into low and high frequency bands as shown in Figure 4.

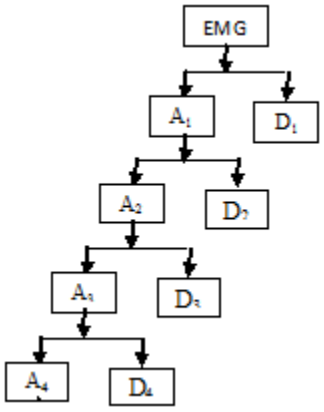

Figure 4: Decomposition of input signal into multiple levels.

The input EMG signal is split into low and high frequency bands. The low frequency filter coefficients or approximations, $W_{\psi}(n) = \sum_{k=o}^{N-1} d(k)\psi(n-k)$ (5)

mother wavelet, $\psi(n) = \frac{1}{\sqrt{2^j}}\psi(\frac{n-k2^j}{2})$ j and k are shift parameters (6)

The high frequency filter coefficients or details, $W_{\varphi}(n) = \sum_{k=o}^{N-1} d(k)\varphi(n-k)$ (7)

The coefficients of all the levels contain significant amplitude and considered for further analysis. The statistical features are extracted from the detailed and approximation coefficients of each of the n-levels.

d) Wavelet Packet Transform:

The WPT can generate a superfluous set of subspaces arranged in a binary tree structure with any desired resolution, allowing the input signal to be decomposed. The wavelet packet tree for EMG signal after performing 7-level decomposition is shown in Figure 5. It consists of 2^7=128 frequency sub bands.

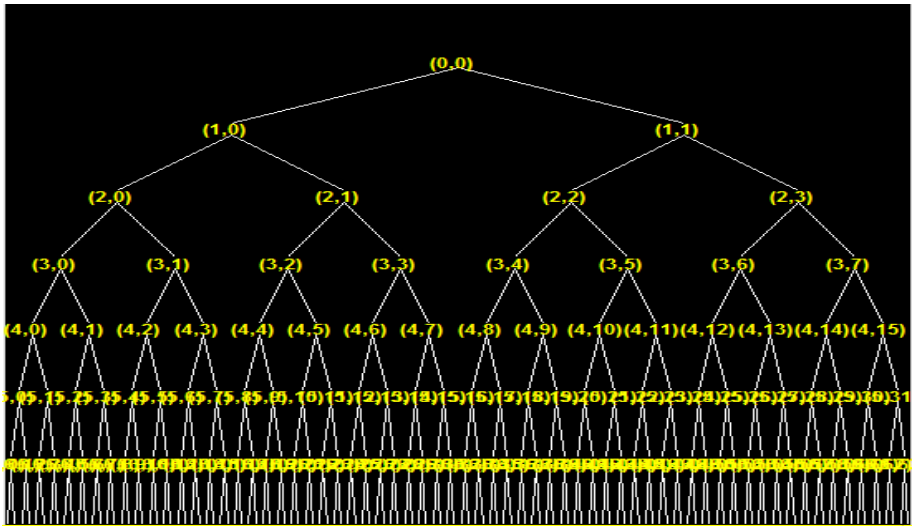

Figure 5 Wavelet Packet Tree for 7 levels

The maximum possible frequency for the signal, according to the Nyquist theorem, would be $f_s/2$ where $f_s$is the sampling frequency. Frequency bands corresponding to five decomposition levels and their corresponding sampling frequencies and nodes are listed in Table I.

Table 1 Frequency ranges for different levels

Node	F (Hz)	f_s	Node	F (Hz)	f_s	Node	F (Hz)	f_s
(1,0)	0.00390	0-500	(4,7)	0.08593	437.5-500	(5,12)	0.1679	375-406.25
(1,1)	0.00781	500-1000	(4,8)	0.08984	500-562.5	(5,13)	0.1718	406.25-437.5
(2,0)	0.01171	0-250	(4,9)	0.09375	562.5-625	(5,14)	0.1757	437.5-468.75
(2,1)	0.01562	250-500	(4,10)	0.09765	625-687.5	(5,15)	0.1796	468.75-500
(2,2)	0.01953	500-750	(4,11)	0.10156	687.5-750	(5,16)	0.1835	500-531.25
(2,3)	0.02343	750-1000	(4,12)	0.10546	750-812.5	(5,17)	0.1875	531.25-562.5
(3,0)	0.02734	0-125	(4,13)	0.10937	812.5-875	(5,18)	0.1914	562.5-593.75
(3,1)	0.03125	125-250	(4,14)	0.11328	875-937.5	(5,19)	0.1953	593.75-625
(3,2)	0.03515	250-375	(4,15)	0.11718	937.5-1000	(5,20)	0.1992	625-656.25
(3,3)	0.03906	375-500	(5,0)	0.12109	0-31.25	(5,21)	0.2031	656.25-687.5
(3,4)	0.04296	500-625	(5,1)	0.125	31.25-62.5	(5,22)	0.2070	687.5-718.75
(3,5)	0.04687	625-750	(5,2)	0.12890	62.5-93.75	(5,23)	0.2109	718.75-750
(3,6)	0.05078	750-875	(5,3)	0.13281	93.75-125	(5,24)	0.2148	750-781.25
(3,7)	0.05468	875-1000	(5,4)	0.13671	125-156.25	(5,25)	0.2187	781.25-812.5
(4,0)	0.05859	0-62.5	(5,5)	0.14062	156.25-187.5	(5,26)	0.2226	812.5-843.75
(4,1)	0.0625	62.5-125	(5,6)	0.14453	187.5-218.75	(5,27)	0.2265	843.75-875
(4,2)	0.06640	125-187.5	(5,7)	0.14843	218.75-250	(5,28)	0.2304	875-906.25
(4,3)	0.07031	187.5-250	(5,8)	0.15234	250-281.25	(5,29)	0.2343	906.25-937.5
(4,4)	0.07421	250-312.5	(5,9)	0.15625	281.25-312.5	(5,30)	0.2382	937.5-968.75
(4,5)	0.07812	312.5-375	(5,10)	0.16015	312.5-343.75	(5,31)	0.2421	968.75-1000
(4,6)	0.08203	375-437.5	(5,11)	0.16406	343.75-375			

3.Feature extraction algorithm:

The significant features of the signal are extracted using the following algorithm. The important steps involved in this are summerized below:

Step 1 : Perform wavelet decomposition using DWT and WPT

Step 2 : Compute the statistical features such as energy, entropy, standard deviation and mean for the wavelet coefficients in each level.

a) Energy: According to Parseval's theorem, the energy of the signal can be segregated at different resolution level. For approximation coefficients, $E_{ai}(i) = \sum_{j=1}^{N} \left| a_{ij}(i) \right|^2, i = 1,2,.....,l$ (8)

For detailed coefficients, $E_{di}(i) = \sum_{j=1}^{N} \left| d_{ij}(i) \right|^2, i = 1,2,.....,l$ (9)

b) Entropy: Entropy in the EMG is a measure of microstates. The more microstates, i.e. more chaos and entropy, the more complexity in the EMG and more promising patterns. The entropy of approximations and details respectively are given by,

$$P_{ai}(i) = -\sum_{j=0}^{N-1} P[a_{ij}(i)] \log_2 P[(a_{ij}(i)] \quad (10)$$

$$P_{di}(i) = -\sum_{j=0}^{N-1} P[d_{ij}(i)] \log_2 P[d_{ij}(i)] \quad (11)$$

c) Mean: This parameter articulates the strength of muscle for which we are analysing EMG and its fortitude excessively. $M_{ai}(i) = \frac{1}{N} \sum_{j=1}^{N} a_{ij}(i),\ M_{di}(i) = \frac{1}{N} \sum_{j=1}^{N} d_{ij}(i)$ (12)

d) Standard deviation: $S_{ai}(i) = \sqrt{\frac{1}{N} \sum_{j=1}^{N} [a_{ij}(i) - M_i)^2},\ S_{di}(i) = \sqrt{\frac{1}{N} \sum_{j=1}^{N} [d_{ij}(i) - M_i]^2}$ (13)

Step 3: Find the maximum value of the features for each decomposition level.

Maximum Energy, $E_{mi}(i) = \max\{E_{ai}, E_{di}\}, i = 1,2,.....,l$ (14)

Maximum entropy, $P_{mi}(i) = \max\{P_{ai}, P_{di}\}, i = 1,2,.....,l$ (15)

Maximum mean, $$M_{mi}(i) = \max\{M_{ai}, M_{di}\}, i = 1,2,.....,l \quad (16)$$

Maximum standard deviation, $$S_{mi}(i) = \max\{S_{ai}, S_{di}\}, i = 1,2,.....,l \quad (17)$$

The frequency band of each scale [$f_m/2$: f_m] of the DWT/WPT is allied to the sampling rate of the original signal, given by $f_m=f_s/2l+1$, where f_s is the sampling frequency, and l is the level of decomposition. In this study, the sampling frequency of the EMG signal is set to be 1000 Hz.

Step 4: Find the first and second derivatives of the feature vectors.

First Derivatives (FD): The first derivative measures the rate of change between the successive and predecessor values. Given that there are some features extracted from the same kind of finger motion, these feature sets should have relation among neighborhood samples. These signals are all decomposed to obtain the same frequency scales by wavelet transform. The correlation between different frequency regions has been indorsed as a sort of effective characteristic of the signal. First Derivatives (FD) and Second Derivatives (SD) are used to analyse the correlation. The FD-based features are obtained by finding the first order derivative of the features, i.e.

$$FD - Energy(FDE) = \nabla E_{mt}(i) = E_{m(t+1)}(i) - E_{m(t-1)}(i) \quad (18)$$

$$FD - Entropy(FDP) = \nabla P_{mt}(i) = P_{m(t+1)}(i) - P_{m(t-1)}(i) \quad (19)$$

$$FD - Mean(FDM) = \nabla M_{mt}(i) = M_{m(t+1)}(i) - M_{m(t-1)}(i) \quad (20)$$

$$FD - Std(FDS) = \nabla S_{mt}(i) = S_{m(t+1)}(i) - S_{m(t-1)}(i) \quad (21)$$

Second Derivative (SD): The SD feature vector contains the details regarding the changes or movements.

$$SD - Energy(SDE) = \nabla^2 E_{mt}(i) = E_{m(t+1)}(i) - 2E_{mt}(i) + E_{m(t-1)}(i) \quad (22)$$

$$SD - Entropy((SDP) = \nabla^2 P_{mt}(i) = P_{m(t+1)}(i) - 2P_{mt}(i) + P_{m(t-1)}(i) \quad (23)$$

$$SD - Std(SDS) = \nabla^2 S_{mt}(i) = S_{m(t+1)}(i) - 2S_{mt}(i) + S_{m(t-1)}(i) \quad (24)$$

$$SD - Mean(SDM) = \nabla^2 M_{mt}(i) = M_{m(t+1)}(i) - 2M_{mt}(i) + M_{m(t-1)}(i) \quad (25)$$

Step 5: The above mentioned feature vectors can be concatenated to afford new feature vectors with more information. Table 2 shows the set of features used for classifications.

Table 2 Set of features using DWT and WPT

Features	Static	Dynamic		Fused features
		First Derivative	Second Derivative	
Energy	E	FDE	SDE	[E FDE SDE]
Entropy	P	FDP	SDP	[P FDP SDP]
Mean	M	FDM	SDM	[M FDM SDM]
Standard Deviation	S	FDS	SDS	[S FDS SDS]

ANN based Classification

Pattern recognition techniques are necessary for the classification of EMG signals. . Pattern recognition is the process of realizing a pattern of a given object based on the knowledge already possessed [39].This work investigates the performance of FFNN and CFNN in finger movement classification. Both the networks were trained using Levenberg-Marquardt Back Propagation (LMBP) algorithm. This algorithm's performance function is represented in the form of sum of squares and the Hessian matrix , given by $H = J^T J$ and the gradient is $g = J^T e$, where J is the Jacobian matrix and e is the vector of network errors. The training algorithm uses approximate Hessian matrix $x_{k+1=}x_k - [J^T J + \mu I]^{-1} J^T e$. The CFNN and FFNN are identical in that they both have a weight link from the input to each layer and from each layer to the layers that follow. Each layer of neurons in a cascade connection is associated with every layer of neurons before it. If there are enough hidden neurons, this network can learn any input-output relationship. The network is shown in figure 6.

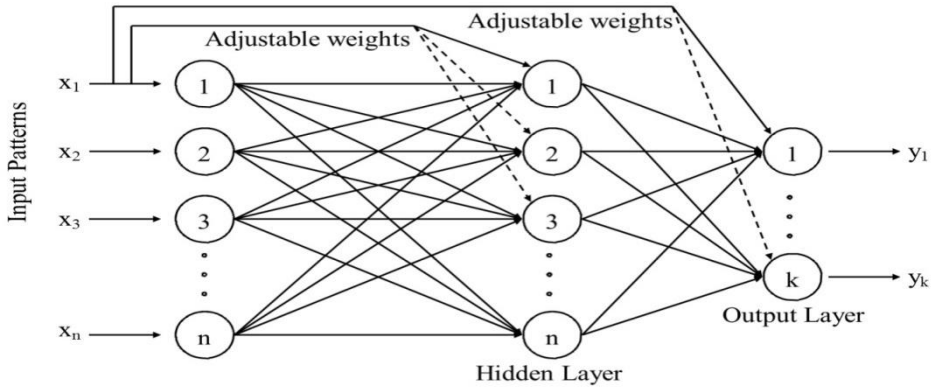

Figure 6 Cascaded Feed Forward ANN

The following is a description of the key steps in the learning CFNN algorithm:

Step 1: Train the net using the necessary input and output units until the error is at its lowest possible level.

Step 2: compute the residual error, $E_j(p) = [y_j(p) - t_j(p)]y_j(p)'$ for $j = 1,2,....m$ and average residual error, $E_{avj}(p) = (1/P)\sum_{p=1}^{P} E_j(p)$ for each training pattern p, where $y_j(p)$ and $t_j(p)$ is output and target vector respectively for input vector $x_j(p)$.

Step 3: Add first hidden unit.

Step 4: Each input unit is connected to a candidate unit X, and initialize the weights from the input units to X (but is not connected to the output units). To increase correlation C, train these weights.

$$C = \sum_{j=1}^{m} \left| \sum_{p=1}^{P} [z(p) - z_{av}(E_j(p) - E_{avj}(p)] \right| \tag{26}$$

where $z(p)$ is the average activation over all patterns $p = 1,2,....P$.

$$z_{av} = \frac{1}{P}\sum_{p=1}^{P} z(p) \tag{27}$$

Step 5: All the weights should be trained to the output units. Stop when the permissible error or the maximum number of units is achieved. If not, move on to step 6.

Step 6: When the stopping condition is false, perform steps 7 and 8.

Step 7: Each input unit and previously added hidden unit is coupled to a candidate unit X. To increase C, train with these weights.

Step 8: All the weights should be trained to the output units. If the maximum number of units or the allowable error has been reached, stop; otherwise, continue the previous steps.

4 RESULTS AND DISCUSSION

The EMG information is gathered from several subjects. Each finger motion resulted in the acquisition of 20,000 data points in total. Due to sensor placement and other background disturbances, there is a chance that noises will be added to the signal as it is being captured. In order to analyse the performances, the signal to interference ratio was found after the signal had been pre-processed using the denoising techniques outlined in section 3 (SIR). *SIR= (P/I+N),* where *P* is the Power of input signal, *I* is the power of interfering signal and *N* is random noise. Moreover, the selection of an appropriate wavelet family is an essential step to build a good representative of the signal for contributing to the feature vector. We tested different wavelets such as 'db', 'coif', 'sym' wavelets respectively. For evaluating the performance of denoised EMG signals, three wavelet functions and four soft thresholding methods were taken into consideration. Table 3 shows the SIR values using different wavelet families for different finger movements.

Table 3 Comparison of SIR using various denoising techniques

	db4				coif5				sym4			
	Rig	He	sqrt	Min	Rig	He	sqrt	Min	Rig	He	sqrt	Mini
L1	5.87	***7.4***	5.8	6.8	6.2	**7.3**	6.08	7.03	5.9	7.2	5.84	6.81
L2	5.43	**7.7**	6.1	6.7	5.4	***7.9***	6.85	7.13	5.1	7.5	6.33	6.72
R1	5.55	**8.5**	5.6	7.9	6.2	***9.0***	5.84	8.20	5.5	8.4	5.41	7.74
R2	5.41	7.4	5.6	**7.9**	5.8	7.7	6.12	7.84	5.5	7.4	5.75	***8.30***
M1	5.64	**6.5**	5.6	6.0	5.7	5.6	5.66	**6.38**	5.6	6.5	***6.91***	6.20
M2	6. 14	**6.6**	5.8	6.0	6.6	5.9	5.94	**6.63**	6.5	6.3	***6.79***	6.14
I1	6.42	6.3	5.8	**7.3**	6.0	6.3	6.03	**7.40**	6.5	6.2	***7.41***	7.40
I2	6.05	**9.5**	6.6	8.5	6.4	***9.7***	7.12	8.77	6.0	9.6	6.71	8.57
T1	5.20	7.3	5.3	**8.6**	5.4	7.9	5.47	**8.94**	5.2	7.2	5.31	***9.33***
T2	5.57	**8.0**	5.3	7.6	5.8	***8.1***	5.67	8.05	5.5	7.5	5.29	7.75
TL	5.56	**8.7**	5.8	7.2	5.7	5.6	5.95	**7.60**	5.4	8.7	*8.89*	7.24
TL	6.06	**7.2**	5.9	6.8	6.3	***7.6***	6.54	6.90	6.0	7.3	6.11	6.71
TR	5.04	**7.6**	4.9	7.0	5.3	4.9	5.20	**7.39**	5.0	7.4	*7.97*	6.88
TR	5.31	**7.5**	6.0	6.5	5.4	***8.1***	6.55	6.83	5.2	7.4	6.17	6.26
TM	3.75	5.4	4.3	**5.8**	3.8	6.0	4.52	***6.55***	3.8	5.6	4.41	6.11
TM	4.22	5.9	4.3	**6.7**	4.5	6.4	4.55	6.84	4.3	6.0	4.42	***7.21***
TI1	5.10	7.5	6.0	**9.1**	5.8	7.8	6.40	**9.28**	5.5	7.6	6.03	***9.45***
TI2	6.58	**9.0**	6.7	8.5	7.2	***9.1***	6.98	8.64	6.7	8.8	6.54	8.37
HC	5.87	4.9	**6.0**	5.2	5.8	4.8	4.69	**5.96**	5.5	6.0	***6.35***	5.50
HC	5.96	**6.0**	5.2	5.7	5.1	**6.3**	5.55	6.16	6.0	6.0	***6.43***	5.79
HR	-	14	-	6	-	17	-	3	-	-	12	8
Ov	-	1	-	-	-	7	-	1	-	-	7	4

The best value between a wavelet's thresholding rules is indicated in bold letters in Table 3; the best value between all wavelets is indicated by bold letters with italics. The optimal thresholding rules can be found by comparing SIR performance on denoised EMG data to other thresholding rules. It is found that “coif5” wavelet function gives the best SIR compared to the other two wavelet functions. “Heursure” gives the best results in “coif5” wavelets.

The coiflet wavelets have compactly supported wavelets with the most vanishing moments, and with the function having 2N moments equal to 0 and the scaling function with 2N-1 moments equal to 0. These two functions have a support of length 6N-1. Figure 7 shows the original (blue colour line) and the denoised (red colour line) EMG signal for index, ring and little fingers respectively.

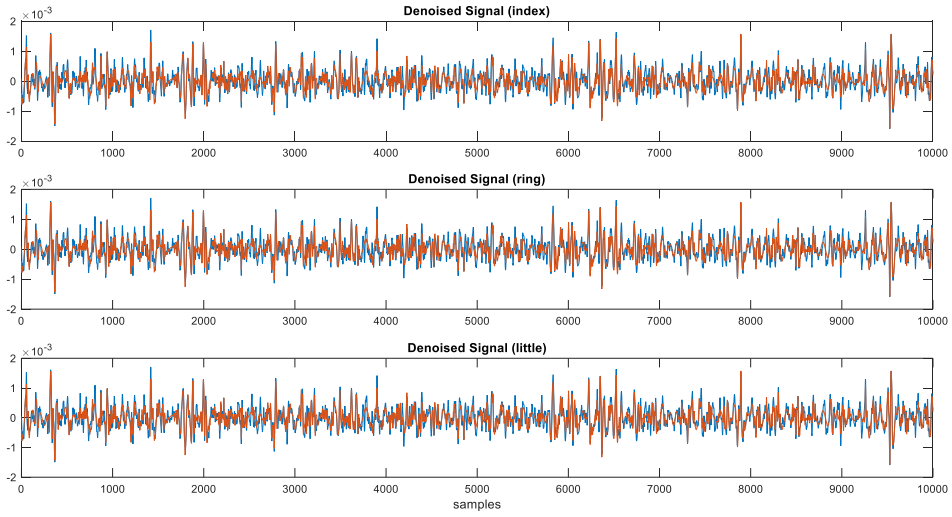

Figure 7 EMG and denoised EMG signal

Thus, coif5 wavelets are considered for further analysis. The denoised signals are decomposed using DWT and WPT. In DWT-based decomposition, only the low frequency bands are divided, consequently producing only two sub-bands in each resolution level. But, WPT produces 2^n sub-bands, where n is the decomposition level .The relevant features are extracted from each sub-band using feature extraction algorithm. The statistical features such as energy, entropy, mean and standard deviation of the signal for each sub-band and further, maximum of these values were computed. Table 4 shows the feature values obtained for one of the finger (little) movements using WPT-based

decomposition. For 7 levels, 27=128 sub-bands are obtained. Out of this, only 7 sub-bands are selected and the corresponding nodes with the sampling frequencies are depicted in column 2 and 4.

Table 4 Resolution levels and corresponding features

Levels	Nodes	Frequency bands (Hz)	Sampling Frequency	Energy	Entropy	Mean	Standard deviation
2	(1,0)	0.003906	0-500	0.048767	4.04E-05	2.13E-05	0.048767
3	(2,0)	0.011719	0-250	88.73588	0.04705	5.72E-05	3.01E-05
4	(3,0)	0.027344	0-125	89.01115	0.045351	8.09E-05	4.27E-05
5	(4,4)	0.074219	250-312.5	94.68076	0	1.26E-11	2.04E-09
6	(5,0)	0.121094	0-31.25	92.20418	0.042083	0.000161	8.69E-05
6	(5,8)	0.152344	250-281.25	98.01157	0	3.61E-11	2.85E-09
6	(5,16)	0.183594	500-531.25	93.92627	0	1.15E-12	1.67E-10
7	(6,16)	0.308594	250-265.625	99.16578	0	1.03E-10	4.10E-09

Similarly, suitable features are extracted for all EMG signals relating to the other finger movements. The first and second derivatives of the feature set are also obtained and new feature vectors are formed.. The back propagation neural networks are used for classifying 10 types of finger movements. The samples are divided into 3 sets: 70% for training, 15%for validation and15% for testing. The classification accuracy achieved for different sets of features is shown in Table 5. In all the cases, both DWT and WPT-based features produces more than 80% of classification accuracy (for FFNN and CFNN). It is also obvious that the classification accuracy is improved by using CFNN.

Table 5 Classification accuracy using FFNN and CFNN classifiers

	Features	DWT		WPT	
		FFNN	CFNN	FFNN	CFNN
Energy	E	83.9720	82.1726	81.9893	82.9726
	FDE	82.8724	84.9387	82.7249	85.3387
	SDE	81.9893	83.6055	81.6893	83.9054
Entropy	P	82.0060	81.9977	82.1060	83.7712
	FDP	82.4892	82.1143	83.8924	84.0143
	SDP	81.9977	82.0060	82.9077	83.9060
Standard	S	81.9893	82.9893	81.1293	82.6873
	FDP	83.7887	84.0060	84.8875	85.1060

deviation	SDP	81.9893	83.4389	82.9193	83.4389
Mean	M	82.3392	83.9803	82.0392	83.9803
	FDM	83.4055	84.0893	83.2059	84.0893
	SDM	81.9893	82.1895	82.3893	85.9898

The percentage of classification is further improved by means of fused features, i.e., the concatenation of the first and second order derivatives of the feature sets. The classification accuracy achieved for the fused features is shown in Table 6. It is noticed that the classification rate is improved to more than 15% in most of the cases, i.e., greater than 95% is obtained. It is also observed that the energy-based feature set produced the promising results, i.e. ~98% for both the classifiers.

Table 6 Classification accuracy using fused features

		DWT		WPT	
	Features	FFNN	CFNN	FFNN	CFNN
Energy	[E FDE SDE]	**98.95008**	**98.3361**	**97.3378**	**98.5857**
Entropy	[P FDP SDP]	95.2579	95.4243	96.0899	97.7573
Standard deviation	[S FDS SDS]	96.2562	97.9201	94.5092	97.8369
Mean	[M FDM SDM]	96.9501	93.0116	96.5890	98.0033

Tables7 and 8illustratethe confusion matrices of the classification results across all subjects with fused energy-based features i.e, [W FDE SDE] using FFNN and CFNN classifiers. Let C_1, C_2, C_3, C_4, C_5, C_6, C_7, C_8, C_9 and C_{10} denote classes for Hand Close (HC), Thumb (T), Index (I), Little(L), Middle(M), Ring(R), Thumb-Index(TI), Thumb-Middle(TM), Thumb-Ring(TR) and Thumb-Little(TL) respectively. The diagonal elements show the correctly classified finger movements in percentage and off-diagonal elements give the mis-classified one.

Table 7 Confusion matrix of the classification results using DWT-FFNN using energy and it's derivatives

	C1	C2	C3	C4	C5	C6	C7	C8	C9	C10
C1	0.99	0.00	0.01	0.04	0.00	0.02	0.01	0.00	0.01	0.00
C2	0.00	0.99	0.01	0.04	0.01	0.00	0.00	0.00	0.01	0.10

C3	0.00	0.00	0.98	0.00	0.01	0.00	0.01	0.02	0.00	0.01
C4	0.00	0.01	0.00	0.99	0.00	0.00	0.01	0.00	0.00	0.00
C5	0.00	0.00	0.01	0.01	0.98	0.00	0.01	0.01	0.00	0.04
C6	0.01	0.00	0.00	0.01	0.00	0.99	0.00	0.00	0.01	0.00
C7	0.00	0.01	0.01	0.00	0.00	0.00	0.98	0.01	0.00	0.00
C8	0.00	0.00	0.00	0.00	0.01	0.00	0.00	0.99	0.01	0.01
C9	0.01	0.00	0.01	0.02	0.00	0.01	0.04	0.01	0.98	0.00
C10	0.00	0.01	0.00	0.01	0.00	0.00	0.01	0.00	0.01	0.99

Table 8Confusion matrix of the classification results using DWT-CFNN using energy and it's derivatives

	C1	C2	C3	C4	C5	C6	C7	C8	C9	C10
C1	0.98	0.00	0.00	0.07	0.00	0.00	0.00	0.00	0.01	0.00
C2	0.00	0.99	0.00	0.00	0.02	0.00	0.00	0.00	0.00	0.00
C3	0.00	0.00	0.98	0.01	0.00	0.00	0.00	0.00	0.00	0.01
C4	0.00	0.00	0.00	0.99	0.00	0.00	0.00	0.00	0.00	0.00
C5	0.00	0.00	0.00	0.02	0.98	0.00	0.00	0.00	0.00	0.00
C6	0.00	0.00	0.00	0.01	0.02	0.99	0.00	0.00	0.01	0.00
C7	0.00	0.00	0.01	0.01	0.00	0.00	0.98	0.00	0.00	0.00
C8	0.00	0.00	0.00	0.04	0.00	0.00	0.00	0.96	0.02	0.00
C9	0.00	0.00	0.00	0.05	0.03	0.01	0.00	0.00	0.99	0.01
C10	0.00	0.00	0.00	0.00	0.00	0.00	0.00	0.00	0.01	0.99

Comparing Tables 7 and 8, the feature set [E FDE SDE] with CFNN classifier gives the average highest classification rate i.e., 98.58%. The error histogram of the network, which is shown in Figure 8, provides extra details for assessing the effectiveness of the trained network by showing the distribution of the residuals between targets and network output. It is shown in this case that most of

the error lies between -1.5and1.5. The histogram has the capability of indicating the outliers. Nevertheless, there is a learning point with an error of 0.053.

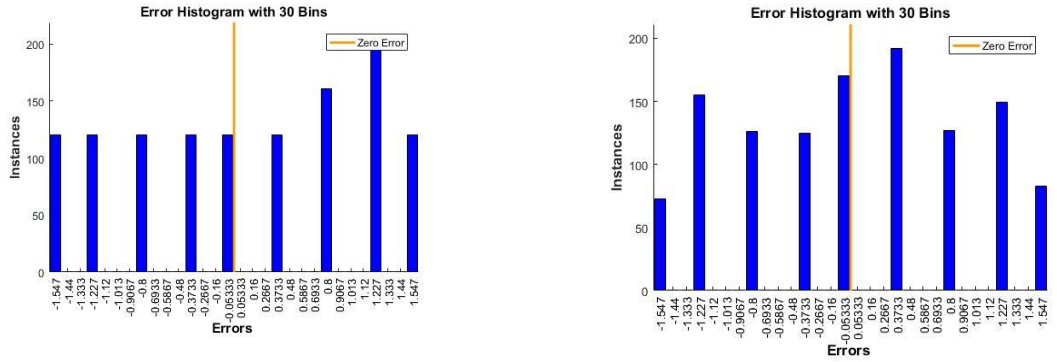

(a) (b)

Figure 8 Error Histogram plots for different sets of training and classifiers (a) DWT-FFNN-Energy and it's derivatives (b) DWT-CFNN-Energy and it's derivatives

The proposed framework for finger motion classification is compared with other state-of-the-art methods in literature and the results are shown in Table 8

Table 8 Comparison of classification accuracy of the proposed work with the existing methods

Reference	Features	Classifier	Classification accuracy
Riilloet.al[14]	Mean(M),Root Mean Square(RMS), Willison amplitude(WA),Slope sign change (SSC), Simple Square Integral (SSI), Variance (V),Waveform length (WL)	FFNN	88.81±6.58%
Iker Mesa et.al[17]	Log detector, MAV, median absolute value, variance, zero crossing, mean absolute difference value amplitude of Wilson, histogram Wavelet coefficients and AR coefficients	SVM	86.4%
An-Chih Tsai et al [19]	STFT-Ranking coefficients	SVM	93.9%
Rami N Khushaba et al [20]	Spectral moment derivations in the time domain	SVM	92%

Paul McCool et.al [30]	FFT coefficients	LDA	90.2%
ErcanGokgozet.al[31]	Mean, average power and standard deviation using DWT	Random forest	96.67%
YinaGuo et al [34]	Empirical mode decomposition(EMD) Coefficients	Flexible Neural Tree (FNT)	97.6%
Proposed work	Energy and derivatives using DWT Entropy and derivatives using DWT Standard deviation and derivatives using DWT Mean and derivatives using DWT	FFNN	**98.95008%** **95.2579%** **96.2562%** **96.9501%**
	Energy and derivatives using DWT Entropy and derivatives using DWT Standard deviation and derivatives using DWT Mean and derivatives using DWT	CFNN	**98.3361%** **95.4243%** **97.9201%** **93.0116%**
	Energy and derivatives using WPT Entropy and derivatives using WPT Standard deviation and derivatives using WPT Mean and derivatives using WPT	FFNN	**97.3378%** **96.0899%** **94.5092%** **96.5890%**
	Energy and derivatives using WPT Entropy and derivatives using WPT Standard deviation and derivatives using WPT Mean and derivatives using WPT	CFNN	**98.5857%** **97.7573%** **97.8369%** **98.0033%**

These results revealed the effectiveness of the present technique of separately evaluating statistical information of the performed experimental protocol both in DWT and WPT. More

promising results are obtained for the present study and suggests that the EMG wavelet-based features information for finger motion analysis should have a major attention.

5. CONCLUSION

In this study, we have found out significant consistency among de-noising , decomposition methods and classifiers which are proved by the simulation results. The contribution of this study is to classify finger motions using an efficient ANN-based pattern recognition system and DWT/WPT decomposition method with Heursure de-noising. Wavelet-based denoising method is proposed to remove the artefacts present in the EMG signal. In order to identify the performance of denoising, performance measures in terms of SIR were investigated and the results are discussed and it is concluded that the coiflet wavelet and Heursure threshold rule give the best results. We presented the classification accuracy using fused mean, standard deviation and entropy features. This study achieved significantly better performance by using the combined effect of Heursure denoising and wavelet Energy derivatives. The fused energy features and FFNN/CFNN classifier with Heursure de-noising can be helpful to the clinician for assessing muscle fatigue.

Acknowledgments

The authors thank the volunteers who took part in the trials for their participation and patience.

Funding

The authors declare that no funds, grants, or other support were received during the preparation of this manuscript

Competing Interests

Authors declare no conflict of interest.

Author Contributions

Research concept and drafted the article [Mary Vasanthi S].

Supervised, data analysis and interpretation [Jayasree T].

Data collection and edited the paper [Haiter Lenin A].

All authors read and approve the final manuscript.

Data availability

All data generated or analysed during this study are included within this article

REFERENCES

1 Stifani, N. (2014). Motor neurons and the generation of spinal motor neuron diversity. Frontiers in cellular neuroscience, 8, 293. doi.org/10.3389/fncel.2014.00293

2 Mota, J. A., Gerstner, G. R., & Giuliani, H. K. (2019). Motor unit properties of rapid force development during explosive contractions. The Journal of Physiology, 597(9), 2335. doi: 10.1113/JP277905

3 Phinyomark, A., Quaine, F., Charbonnier, S., Serviere, C., Tarpin-Bernard, F., & Laurillau, Y. (2013). A feasibility study on the use of anthropometric variables to make muscle–computer interface more practical. Engineering Applications of Artificial Intelligence, 26(7), 1681-1688. DOI:10.1016/j.engappai.2013.01.004

4 Asghar A, Jawaid Khan S, Azim F, Shakeel CS, Hussain A, Niazi IK. (2022) Review on electromyography based intention for upper limb control using pattern recognition for human-machine interaction. Proceedings of the Institution of Mechanical Engineers, Part H: Journal of Engineering in Medicine. 236 (5):628-645. doi:10.1177/09544119221074770

5 Falcari, T., Saotome, O., Pires, R., & Campo, A. B. (2020). Evaluation of multi-class support-vector machines strategies and kernel adjustment levels in hand posture recognition by analyzing sEMG signals acquired from a wearable device. Biomedical Engineering Letters, 10(2), 275-284.doi: 10.1007/s13534-019-00141-9.

6 Zhang, X., & Zhou, P. (2012). High-density myoelectric pattern recognition toward improved stroke rehabilitation. IEEE Transactions on Biomedical Engineering, 59(6), 1649-1657. DOI: 10.1109/TBME.2012.2191551

7 Tufan, K. (2013). Noninvasive diagnosis of atherosclerosis by using empirical mode decomposition, singular spectral analysis, and support vector machines. Biomedical Research (0970-938X), 24(3).

8 Vidovic, M. M. C., Hwang, H. J., Amsüss, S., Hahne, J. M., Farina, D., & Müller, K. R. (2015). Improving the robustness of myoelectric pattern recognition for upper limb prostheses by covariate shift adaptation. IEEE Transactions on Neural Systems and Rehabilitation Engineering, 24(9), 961-970. DOI: 10.1109/TNSRE.2015.2492619

9 Hartwell, A., Kadirkamanathan, V., & Anderson, S. (2016, August). Person-specific gesture set selection for optimised movement classification from EMG signals. In 2016 38th Annual International Conference of the IEEE Engineering in Medicine and Biology Society (EMBC) (pp. 880-883). IEEE. doi.org/10.1109/EMBC.2016.7590841

10 Liu, L., Liu, P., Clancy, E. A., Scheme, E., & Englehart, K. B. (2013). Electromyogram whitening for improved classification accuracy in upper limb prosthesis control. IEEE Transactions on Neural Systems and Rehabilitation Engineering, 21(5), 767-774. Doi: 10.1109/TNSRE.2013.2243470

11 Hahne, J. M., Graimann, B., & Muller, K. R. (2012). Spatial filtering for robust myoelectric control. IEEE Transactions on Biomedical Engineering, 59(5), 1436-1443. DOI: 10.1109/TBME.2012.2188799

12 Yang, D., Zhang, H., Gu, Y., & Liu, H. (2017). Accurate EMG onset detection in pathological, weak and noisy myoelectric signals. Biomedical Signal Processing and Control, 33, 306-315. doi.org/10.1016/j.bspc.2016.12.014

13 Verma, N., & Verma, A. K. (2012). Performance analysis of wavelet thresholding methods in denoising of audio signals of some Indian Musical Instruments. Int. J. Eng. Sci. Technol, 4(5), 2040-2045.

14 Haiter Lenin, A., Mary Vasanthi, S, Jayasree, T. (2020) Automated Recognition of Hand Grasps Using Electromyography Signal Based on LWT and DTCWT of Wavelet Energy. International Journal of Computational Intelligence Systems,13(1), 1027–1035. doi.or g/10.2991/ijcis.d.200724.001.

15 Riillo, F., Quitadamo, L. R., Cavrini, F., Gruppioni, E., Pinto, C. A., Pastò, N. C., & Saggio, G. (2014). Optimization of EMG-based hand gesture recognition: Supervised vs. unsupervised data preprocessing on healthy subjects and transradial amputees. Biomedical Signal Processing and Control, 14, 117-125. doi.org/10.1016/j.bspc.2014.07.007

16 Wang, N., Chen, Y., & Zhang, X. (2014). Realtime recognition of multi-finger prehensile gestures. Biomedical Signal Processing and Control, 13, 262-269. doi.org/10.1016/j.bspc.2014.05.007

17 Khushaba, R. N., Al-Timemy, A., Kodagoda, S., & Nazarpour, K. (2016). Combined influence of forearm orientation and muscular contraction on EMG pattern recognition. Expert Systems with Applications, 61, 154-161. doi.org/10.1016/j.eswa.2016.05.031

18 Mesa, I., Rubio, A., Tubia, I., De No, J., & Diaz, J. (2014). Channel and feature

selection for a surface electromyographic pattern recognition task. Expert Systems with Applications, 41(11), 5190-5200. doi.org/10.1016/j.eswa.2014.03.014

19 Ma, Y., Shi, W., Peng, C. K., & Yang, A. C. (2018). Nonlinear dynamical analysis of sleep electroencephalography using fractal and entropy approaches. Sleep medicine reviews, 37, 85-93.

20 Prashar, N., Sood, M., & Jain, S. (2020). Dual-tree complex wavelet transform technique-based optimal threshold tuning system to deliver denoised ECG signal. Transactions of the Institute of Measurement and Control, 42(4), 854-869. doi:10.1177/0142331219895708.

21 Tsai, A. C., Luh, J. J., & Lin, T. T. (2015). A novel STFT-ranking feature of multi-channel EMG for motion pattern recognition. Expert Systems with Applications, 42(7), 3327-3341. doi.org/10.1016/j.eswa.2014.11.044

22 Khushaba, R. N., Takruri, M., Miro, J. V., & Kodagoda, S. (2014). Towards limb position invariant myoelectric pattern recognition using time-dependent spectral features. Neural Networks, 55, 42-58. doi.org/10.1016/j.neunet.2014.03.010

23 Pan, L., Zhang, D., Liu, J., Sheng, X., & Zhu, X. (2014). Continuous estimation of finger joint angles under different static wrist motions from surface EMG signals. Biomedical Signal Processing and Control, 14, 265-271. doi.org/10.1016/j.bspc.2014.08.004

24 Jiang, X., Merhi, L. K., Xiao, Z. G., & Menon, C. (2017). Exploration of force myography and surface electromyography in hand gesture classification. Medical engineering & physics, 41, 63-73. doi.org/10.1016/j.medengphy.2017.01.015

25 I.Daubechies (1991), Ten lectures on wavelets, CBMS Lecture Notes Series, SIAM.

26 Maier, J., Naber, A., & Ortiz-Catalan, M. (2017). Improved prosthetic control based on myoelectric pattern recognition via wavelet-based de-noising. IEEE Transactions on Neural Systems and Rehabilitation Engineering, 26(2), 506-514.

27 Qiu, Y., Kuang, C., Liu, X., & Tang, L. (2022). Single-Molecule Surface-Enhanced Raman Spectroscopy. Sensors, 22(13), 4889. https://doi.org/10.3390/s22134889.

28 Cai, S., Chen, Y., Huang, S., Wu, Y., Zheng, H., Li, X., & Xie, L. (2019). SVM-based classification of sEMG signals for upper-limb self-rehabilitation training. Frontiers in Neurorobotics, 13, 31. doi.org/10.3389/fnbot.2019.00031

29 Benatti, S., Rovere, G., Bösser, J., Montagna, F., Farella, E., Glaser, H., ... & Benini, L. (2017, June). A sub-10mW real-time implementation for EMG hand gesture recognition

based on a multi-core biomedical SoC. In 2017 7th IEEE International Workshop on Advances in Sensors and Interfaces (IWASI) (pp. 139-144). IEEE. doi: 10.1109/IWASI.2017.7974234.

30 Hu, P., Li, S., Chen, X., Zhang, D., & Zhu, X. (2010, November). A continuous control scheme for multifunctional robotic arm with surface EMG signal. In International Conference on Intelligent Robotics and Applications (pp. 81-91). Springer, Berlin, Heidelberg. https://doi.org/10.1007/978-3-642-16584-9_8.

31 Liu, J., & Zhou, P. (2012). A novel myoelectric pattern recognition strategy for hand function restoration after incomplete cervical spinal cord injury. IEEE transactions on neural systems and rehabilitation engineering, 21(1), 96-103. DOI: 10.1109/TNSRE.2012.2218832

32 McCool, P., Petropoulakis, L., Soraghan, J. J., & Chatlani, N. (2015). Improved pattern recognition classification accuracy for surface myoelectric signals using spectral enhancement. Biomedical Signal Processing and Control, 18, 61-68. doi.org/10.1016/j.bspc.2014.12.001

33 Gokgoz, E., & Subasi, A. (2015). Comparison of decision tree algorithms for EMG signal classification using DWT. Biomedical Signal Processing and Control, 18, 138-144. doi.org/10.1016/j.bspc.2014.12.005

34 AlOmari, F., & Liu, G. (2015). Novel hybrid soft computing pattern recognition system SVM–GAPSO for classification of eight different hand motions. Optik, 126(23), 4757-4762. doi.org/10.1016/j.ijleo.2015.08.170

35 Amsüss, S., Goebel, P. M., Jiang, N., Graimann, B., Paredes, L., & Farina, D. (2013). Self-correcting pattern recognition system of surface EMG signals for upper limb prosthesis control. IEEE Transactions on Biomedical Engineering, 61(4), 1167-1176. DOI: 10.1109/TBME.2013.2296274

36 Nguyen, T. L., & Won, Y. (2015). Sleep snoring detection using multi-layer neural networks. Bio-medical materials and engineering, 26(s1), S1749-S1755. DOI: 10.3233/BME-151475

37 Guo, Y., Naik, G. R., Huang, S., Abraham, A., & Nguyen, H. T. (2015). Nonlinear multiscale Maximal Lyapunov Exponent for accurate myoelectric signal classification. Applied Soft Computing, 36, 633-640. doi.org/10.1016/j.asoc.2015.07.032

38 Gu, Y., Yang, D., Huang, Q., Yang, W., & Liu, H. (2018). Robust EMG pattern recognition in the presence of confounding factors: features, classifiers and adaptive

learning. Expert Systems with Applications, 96, 208-217. doi.org/10.1016/j.eswa.2017.11.049

39 Subasi, A. (2012). Classification of EMG signals using combined features and soft computing techniques. Applied soft computing, 12(8), 2188-2198. doi.org/10.1016/j.asoc.2012.03.035

Supplementary Files

This is a list of supplementary files associated with this preprint. Click to download.

- bibliography.docx